

Simultaneous modelling of movement, measurement error, and observer dependence in double observer distance sampling surveys

Abstract: Wildlife researchers often use detections, non-detections and recorded distances of animals encountered in transect surveys to estimate abundance. However, commonly available distance sampling estimators require that distances to target animals are made without error and that animals are stationary while sampling is being conducted. In practice these requirements are often violated. In this paper, we describe a marginal likelihood framework for estimating abundance from double observer data that can accommodate movement and measurement error. In particular, we suppose that two observers independently detect and record binned distances to observed animal groups, and that they record a binary indicator for whether animals were moving or not. Under this framework, stationary animals are subject to measurement error and moving animals are subject to both movement and measurement error. Integrating over unknown animal locations, we construct a marginal likelihood for detection, movement, and measurement error parameters. Estimates of animal abundance can then be obtained via a modified Horvitz-Thompson-like estimator. Unmodelled heterogeneity in detection probability can potentially be incorporated via observer dependence effects. Using simulation, we show that our approach yields low bias compared to approaches that ignoring movement/measurement error even in presence of considerable detection heterogeneity. We demonstrate our approach on data from a double observer waterfowl helicopter survey.

22 **Key words:** aerial survey, mark-recapture distance sampling, measure-
23 ment error, movement, point independence

24 **1 Introduction**

25 Distance sampling surveys (Burnham et al., 1980; Buckland et al., 2001) are
26 often used to estimate the abundance of wildlife populations. Historically,
27 such surveys were implemented using a single observer who followed a tran-
28 sect line and recorded the perpendicular distance to each detected animal
29 group. Assuming 100% detection on the transect line, models can be fitted
30 to these data that estimate abundance over the surveyed area while account-
31 ing for detection probabilities that decrease with distance from the transect
32 line.

33 More recently, investigators discovered that double observer surveys have
34 some large advantages over single observer surveys. For instance, one can
35 use the detection/non-detection records to relax the assumption of 100%
36 detection on the transect line (Borchers et al., 1998), a crucial development
37 for many species and sampling situations (e.g. aerial surveys). Analysis
38 of double observer distance data is now canonically referred to as “mark-
39 recapture distance sampling” (MRDS) because there is a detection history
40 (i.e. binary detection/nondetection records for each observer) in addition to
41 recorded distances. Analysis of these histories could potentially be done in
42 a similar manner to a two sample mark-recapture experiment, although this

43 approach ignores some additional information contained in the distribution
44 of observed distances (Laake and Borchers, 2004).

45 Several different observer configurations are possible within an MRDS
46 estimation framework (Burt et al., 2014). In an “independent” configura-
47 tion, observers search for animals independently. Under this configuration
48 it is possible to try to account for heterogeneity in detection probabilities
49 (e.g. visual distinctiveness of different animal groups) by modelling lack of
50 fit between the distribution of observed distances and estimated detection
51 probabilities as a function of distance (Laake and Borchers, 2004; Borchers
52 et al., 2006; Buckland et al., 2010). The ability to account for such het-
53 erogeneity is important, since abundance estimators are negatively biased
54 otherwise. Alternatively, in a “trial” configuration (Laake and Borchers,
55 2004), one observer searches ahead, while another searches closer to the sur-
56 vey platform. Under this configuration, detections by the first observer are
57 used as trials for the second observer. Collecting data in this manner can be
58 useful for reducing the biasing influence of responsive movement of animals
59 (which often positively biases abundance estimators), but at the cost of no
60 longer being able to model heterogeneity in detection probability (Burt et al.,
61 2014).

62 In this paper, we develop an integrated likelihood framework to account
63 for movement and measurement error within an independent observer MRDS
64 framework. Our objective is to account for the biasing effects of measurement
65 error and responsive movement while also being able to model individual

heterogeneity through an observer dependence specification. The effect of movement on distance sampling estimators has previously been examined by Glennie et al. (2015), who showed movement could cause considerable bias in distance-based abundance estimators. However, we have not found any papers that attempt to explicitly model movement. However, a number of authors have proposed models that account for measurement error in specific distance sampling applications (see e.g. Borchers et al., 2010, and references therein).

The remainder of this article is structured as follows. First, we describe a motivating data set, in which distance, detection histories, and individual covariates are assembled from a double observer waterfowl aerial survey. Second, we describe a maximum marginal likelihood (MML) framework for analyzing these data. Under our framework, animal locations are treated as latent variables. Next, we illustrate our method by analyzing the waterfowl data set and examine estimator performance with two simulation studies. We conclude with a short discussion.

2 Waterfowl data

In June of 2014, biologists conducted a pilot double observer helicopter survey of Arctic bird species in the Queen Maud Gulf Migratory Bird Sanctuary (Nunavut, Canada). The birds surveyed were predominantly waterfowl, but also included cranes and ptarmigan; we refer to them collectively as water-

87 fowl for the remainder of the paper. The purpose of this particular survey
88 was not to estimate abundance over the whole area. Rather, researchers
89 were interested in comparing estimates of detection probability from double
90 observer survey methods to estimates of detection probability using single
91 observer protocols. The survey is described in greater detail elsewhere (Al-
92 isauskas and Conn, 2017), but we briefly provide information relevant to the
93 analysis conducted later in this paper.

94 In the survey, two observers on the same side of the helicopter indepen-
95 dently detected and recorded the perpendicular distance from the transect
96 line to each bird group they observed. Distances were binned into 6 classes:
97 0-40m, 40-80m, 80-120m, 120-160m, 160-200m, and 200m+. They also
98 recorded species, the number of waterfowl in each detected group (“group”),
99 and a binary indicator for whether the waterfowl group was flapping their
100 wings (“moving”). These data were previously analyzed by Alisauskas and
101 Conn (2017), who used standard MRDS methods that ignored movement
102 and measurement error in their analysis. Their analysis suggested higher
103 detection probabilities for moving individuals, larger group sizes, and for the
104 front seat observer (relative to a rear seat observer). They also estimated
105 similar species effects on detection for 7 of the 9 species analyzed; here, we
106 pool detections of these 7 species (Canada goose, king eider, long tailed duck,
107 northern pintail, rock ptarmigan, sandhill crane, and white fronted goose)
108 to form an illustrative dataset. This protocol led to a total of 1025 unique
109 waterfowl group detections; 323 were detected by both observers, 353 by the

front observer only, and 258 by the back observer only. Note that the the
back observer’s view of the first distance bin was partially obstructed. A plot
of observed distance deviations suggests responsive movement away from the
aircraft for moving animal groups. There were also some minor distance dis-
crepancies for animal groups that were not moving, which is suggestive of
measurement error (Fig. 1). Our objective is to build models that formally
account for movement and measurement error processes.

3 Model development

Consider a double observer MRDS survey where observers independently
record binned distances to detected groups of animals and a total of n animal
groups are encountered by at least one observer (see Table 1 for a complete
list of notation). We develop a two stage approach for estimating abundance
in the surveyed area from such data. In the first step, a MML framework
is used to simultaneously estimate parameters of detection, movement, and
measurement error processes. In the second, a Horvitz-Thompson-like es-
timator is used to estimate abundance conditioned on parameter estimates
from step 1 (a bootstrap procedure is used to quantify precision). For pur-
poses of this paper we do not explicitly consider the problem of extrapolating
abundance/density to a larger region (e.g. to unsurveyed locations); we touch
on this issue in the Discussion.

In MRDS surveys with binned distances, observers record animals as

131 occurring in one of $n_{\mathcal{S}}$ perpendicular distance bins, $\mathcal{S} = \mathcal{S}_1, \mathcal{S}_2, \dots, \mathcal{S}_{n_{\mathcal{S}}}$. De-
 132 tection probability typically decreases with distance from the transect line,
 133 and the maximum distance bin is often set such that animals further away
 134 are poorly detected and can be ignored without greatly affecting precision of
 135 abundance estimates. Movement and measurement error introduce compli-
 136 cations: animals can potentially move into or out of \mathcal{S} , and animals outside
 137 of \mathcal{S} can be detected in \mathcal{S} . For these reasons, the models we develop rely
 138 on augmenting \mathcal{S} with additional distance bins to allow for movement and
 139 measurement error (Fig. 2). Call this augmented set \mathcal{Z} .

140 Let y_{oi} be a binary indicator for whether or not the i th animal group was
 141 detected by observer o . Similarly, let d_{oi} denote the distance bin recorded by
 142 observer o for animal group i (note d_{oi} is only defined when $y_{oi} = 1$). Letting
 143 bold lower case symbols denote vectors (e.g. \mathbf{y}_o gives a sequence of detections
 144 for observer o , $i = 1, 2, \dots, n$) and bold upper case symbols denote matrices,
 145 we seek to define a marginal likelihood $[\boldsymbol{\theta} | \mathbf{Y}, \mathbf{D}, \mathbf{X}]$, where $\boldsymbol{\theta} = \{\boldsymbol{\beta}, \boldsymbol{\phi}, \boldsymbol{\varphi}\}$
 146 are parameters describing detection, movement, and measurement error, and
 147 \mathbf{X} include individual covariates collected for each animal group that can be
 148 used to explain variation in detection probabilities.

149 **3.1 Likelihood**

150 To construct such a likelihood, we start with the general framework proposed
 151 by Borchers et al. (2015) for spatial mark-recapture and distance sampling
 152 surveys. Conditioning on detection, Borchers et al. (2015) suggested that

the joint distribution of animal locations and detections could be written as a product of (1) a joint probability density function for the latent locations of animals, and (2) a joint probability mass function for the encounter histories conditional on location. We expand upon this framework to allow movement to affect the distribution of animal locations and to incorporate a measurement error mechanism.

Letting \mathbf{z}_o denote the true locations of animals when they enter the field of view of observer o , we write the joint probability mass function of observed data as a product of

1. $[\mathbf{Z}|\boldsymbol{\theta}]$, a bivariate probability mass function for the distribution of true animal locations, given detection by at least one observer; and
2. $[\mathbf{Y}, \mathbf{D}|\mathbf{Z}, \boldsymbol{\theta}, \mathbf{X}]$, a model for binary detections and observed distances given true unobserved locations and individual detection covariates.

If we knew the true locations of observed animals, we could simply base inference on the likelihood

$$[\boldsymbol{\theta}|\mathbf{Y}, \mathbf{D}, \mathbf{X}] \propto [\mathbf{Z}|\boldsymbol{\theta}][\mathbf{Y}, \mathbf{D}|\mathbf{Z}, \boldsymbol{\theta}, \mathbf{X}].$$

However, we do not know the actual animal locations so instead integrate (sum) over an augmented set of distance bins \mathcal{Z} that could plausibly have resulted in a detection (see *Distribution of animal locations* for more discussion of bin augmentation). As such, we write the joint marginal likelihood

172 of detection, movement, and measurement error parameters as

$$[\boldsymbol{\theta}|\mathbf{Y}, \mathbf{D}, \mathbf{X}] \propto \prod_i \left(\sum_{z_{i1} \in \mathcal{Z}} \sum_{z_{i2} \in \mathcal{Z}} [\mathbf{z}_{i\cdot}|\boldsymbol{\theta}] [\mathbf{y}_{i\cdot}, \mathbf{d}_{i\cdot}|\mathbf{z}_{i\cdot}, \boldsymbol{\theta}, \mathbf{x}_i] \right). \quad (1)$$

173 We now describe each of the likelihood components in further detail.

174 3.1.1 Distribution of animal locations

175 The first component of the likelihood (Eq. 1) is the joint probability mass
 176 function for the locations of group i , $[\mathbf{z}_{i\cdot}|\boldsymbol{\theta}]$ given detection by at least one
 177 observer. We write this distribution as a function of (i) an initial state dis-
 178 tribution, (ii) a movement kernel, and (iii) a thinning probability equivalent
 179 to detection probability by at least one observer. Specifically, we set

$$[\mathbf{z}_{i\cdot}|\boldsymbol{\theta}] \propto [z_{i1}][z_{i2}|z_{i1}, \boldsymbol{\phi}] p_i^*(z_{i1}, z_{i2}|\mathbf{x}_i, \boldsymbol{\beta}, \boldsymbol{\phi}, \boldsymbol{\varphi}). \quad (2)$$

180 We make the assumption that the first observer (typically in a front seat)
 181 detects animal groups before any responsive movement has occurred. Un-
 182 der this assumption, random placement of transect lines should help ensure
 183 that perpendicular distances of animals from the transect line are uniformly
 184 distributed in space (cf. Buckland et al., 2001). Letting π_j denote the pro-
 185 portional diameter of distance bin j (i.e. $\pi_j = a_j / \sum_k a_k$ where a_j is the
 186 diameter of of distance bin j), we simply have

$$[z_{i1}] = \text{Categorical}(\pi_1, \pi_2, \dots, \pi_{n_{\mathcal{Z}}}),$$

187 where it is understood that “Categorical” denotes a multinomial distribution
 188 with index 1, and n_Z is the number of latent distance bins.

189 Next, the bivariate movement pmf $[z_{i2}|z_{i1}, \phi]$ describes the location of
 190 animal group i when it enters the field of view of observer 2 as a function of
 191 the location when it was in the field of view of observer 1. We model this as
 192 another categorical distribution:

$$[z_{i2}|z_{i1}, \phi] = \text{Categorical}(\psi(z_{i1}, 1), \psi(z_{i1}, 2), \dots, \psi(z_{i1}, n_Z)). \quad (3)$$

193 For applications in this paper, we parameterize the movement transition ker-
 194 nel probabilities ψ using asymmetric kernels. Using an asymmetric kernel
 195 can allow movement rates to be different toward and away from the transect
 196 line (anticipating a behavioral response to the survey platform). In particu-
 197 lar, we set

$$198 \quad \psi(z_{i1}, z_{i2}) \propto g(z_{i1}, z_{i2}|\phi), \text{ where} \quad (4)$$

199

$$200 \quad g(z_{i1}, z_{i2}) = \begin{cases} f(\delta_{i2}|\mu = \delta_{i1}, \sigma = \phi_1) & z_{i2} < z_{i1}, m_i = 1 \\ f(\delta_{i2}|\mu = \delta_{i1}, \sigma = \phi_2) & z_{i2} \geq z_{i1}, m_i = 1 \\ 1.0 & z_{i2} = z_{i1}, m_i = 0 \\ 0.0 & z_{i2} \neq z_{i1}, m_i = 0 \end{cases} \quad (5)$$

201 Here, $f()$ gives a probability density function; in our examples, we consider

202 Laplace (double exponential) and Gaussian distributions as choices for $f()$.
 203 Note that δ_{io} gives the perpendicular distance from the transect line to the
 204 midpoint of distance bin z_{io} . Also note that we assume that stationary
 205 animals (i.e. with $m_i = 0$) do not change distance bins.

206 Finally, the thinning probability $p_i^*(z_{i1}, z_{i2} | \mathbf{x}_i, \boldsymbol{\beta}, \boldsymbol{\phi}, \boldsymbol{\varphi})$ describes the prob-
 207 ability of being detected by at least one observer for an animal that is in
 208 distance bin z_{i1} at time 1 and z_{i2} at time 2. For generality, we calculate
 209 probability as the sum of obtaining one of the three possible detection histo-
 210 ries: 11, 10, or 01 (detected by both observers, detected by the front observer
 211 but not the back, or detected by the back observer but not the front). In
 212 particular,

$$\begin{aligned}
 p_i^*(z_{i1}, z_{i2} | \mathbf{x}_i, \boldsymbol{\beta}, \boldsymbol{\phi}, \boldsymbol{\varphi}) &= p_{i1}(z_{i1})\omega(z_{i1}, \mathcal{S})p_{i2}(z_{i2})\omega(z_{i2}, \mathcal{S}) + \\
 &\quad p_{i1}(z_{i1})\omega(z_{i1}, \mathcal{S}) [p_{i2}(z_{i2})(1 - \omega(z_{i2}, \mathcal{S})) + (1 - p_{i2}(z_{i2}))] + \\
 &\quad p_{i2}(z_{i2})\omega(z_{i2}, \mathcal{S}) [p_{i1}(z_{i1})(1 - \omega(z_{i1}, \mathcal{S})) + (1 - p_{i1}(z_{i1}))].
 \end{aligned} \tag{6}$$

213 This expression is slightly different than typically encountered in mark-
 214 recapture calculus, as one must account for two ways of getting a 0 in a
 215 capture history: an observer can miss the animal group, or an observer can
 216 detect the group but determine it is out of the truncation range of the tran-
 217 sect (i.e. $\notin \mathcal{S}$). To account for the latter possibility, we make use of the
 218 measurement error kernel ω , which can be parameterized similarly to $\boldsymbol{\phi}$ (see
 219 Eqs. 4-5). In applications in the paper, we consider use of symmetric kernels

220 (Gaussian or Laplace) with a single dispersion parameter, φ . Our expression
 221 for p_i^* also relies on individual- and observer-dependent detection probabili-
 222 ties, $p_{io}(z_{io})$. In order to impart meaningful variation in detection probability,
 223 it is useful to express these in a regression framework on a logit-linear scale,
 224 such that

$$\text{logit}(\mathbf{p}) = \mathbf{X}\boldsymbol{\beta}. \quad (7)$$

225 Note that we write p_{io} as a function of z_{io} to emphasize that the design matrix
 226 \mathbf{X} will often depend on the latent position of animals.

227 **3.1.2 Likelihood of observed detections**

228 The next component of the the likelihood is $[\mathbf{y}_i, \mathbf{d}_i | \mathbf{z}_i, \boldsymbol{\theta}, \mathbf{x}_i]$, the probability
 229 of observing the particular detection history and distance bin values for ani-
 230 mal group i conditional on animal location. Conditional on detection by at
 231 least one observer, there are again three possible types of encounter histories:
 232 11, 10, or 01. For 11 histories, there are n_S^2 combinations of possible recorded
 233 distance bins; for 10 histories, there are n_S distance bins possible for observer
 234 1; for 01 histories, there are n_S distance bins possible for observer 2. Thus,
 235 we can view $[\mathbf{y}_i, \mathbf{d}_i | \mathbf{z}_i, \boldsymbol{\theta}, \mathbf{x}_i]$ as a multinomial distribution with index 1 and
 236 $n_S^2 + 2n_S$ possible outcomes. The likelihood contribution for a particular

237 animal group i can thus be written as

$$(p_i^*)^{-1} \times \begin{cases} p_{i1}(z_{i1})\omega(z_{i1}, d_{i1})p_{i2}(z_{i2})\omega(z_{i2}, d_{i2}) & \text{if } y_{i1} = y_{i2} = 1 \\ p_{i1}(z_{i1})\omega(z_{i1}, d_{i1}) [p_{i2}(z_{i2})(1 - \omega(z_{i2}, \mathcal{S})) + (1 - p_{i2}(z_{i2}))] & \text{if } y_{i1} = 1, y_{i2} = 0 \\ p_{i2}(z_{i2})\omega(z_{i2}, d_{i2}) [p_{i1}(z_{i1})(1 - \omega(z_{i1}, \mathcal{S})) + (1 - p_{i1}(z_{i1}))] & \text{if } y_{i1} = 0, y_{i2} = 1. \end{cases} \quad (8)$$

238 3.2 Horvitz-Thompson-like abundance estimator

239 Minimizing the negative log-likelihood in Eq. 1 provides marginal maximum
 240 likelihood estimates for detection, movement, and measurement error param-
 241 eters, but does not provide a direct estimate of animal abundance, N . We
 242 developed a Horvitz-Thompson-like procedure to calculate abundance esti-
 243 mates, as is common in distance sampling literature (see e.g. Buckland et al.,
 244 2004). This is especially useful when coping with detection probabilities that
 245 vary as a function of individual detection covariates, as one does not need
 246 to model covariate values for undetected animal groups. For instance, in
 247 standard MRDS applications, one might estimate abundance as

$$\hat{N} = \sum_i g_i / p_i^*.$$

248 However, direct application of this estimator is clearly inappropriate under
 249 movement and measurement error, as it can potentially include animals out-
 250 side of the surveyed area, or include animals that move into the surveyed

251 area.

252 Since distance sampling produces estimates of abundance at a single point
 253 in time, we must first define the time and area for which the estimate ap-
 254 plies before constructing an appropriate estimator. In the case of responsive
 255 movement away from a survey platform, we are likely better off referencing
 256 abundance relative to the position of animals when they enter the field of
 257 view of observer 1 than we are for observer 2. Also, since animals are not
 258 recorded if perceived to be outside of \mathcal{S} , it may be best to limit the scope
 259 of inference to those animals that truly occur in \mathcal{S} . We construct a Horvitz-
 260 Thompson-like estimator for abundance in the surveyed region \mathcal{S} at time 1
 261 as follows:

$$\hat{N}|\boldsymbol{\theta} = \sum_i \sum_{z_{i1} \in \mathcal{S}} \sum_{z_{i2} \in \mathcal{Z}} \frac{g_i \times [\mathbf{z}_i | \boldsymbol{\theta}]}{p_i^*(z_{i1}, z_{i2})}. \quad (9)$$

262 This formulation integrates over the latent position of animal groups at times
 263 1 and 2 with the restriction that the position at time 1 is within \mathcal{S} .

264 To produce estimates of precision and confidence limits, we implemented a
 265 parametric bootstrap procedure. In particular, we approximate the sampling
 266 distribution of parameter estimates as

$$[\boldsymbol{\theta}_{boot}] = \text{Multivariate Normal}(\boldsymbol{\theta}_{MLE}, \boldsymbol{\Sigma}),$$

267 where $\boldsymbol{\Sigma}$ is a covariance matrix calculated as the inverse Hessian matrix
 268 of the likelihood evaluated at the MLE estimates. Then, for each of $k =$

269 $1, 2, \dots, n_{boot}$ replicates, we

- 270 1. Sample $\boldsymbol{\theta}_k \sim [\boldsymbol{\theta}_{boot}]$,
- 271 2. Transform $\boldsymbol{\theta}_k$ into real-scale parameters using inverse link functions,
- 272 3. Calculate \hat{N}_k^{boot} using Eq. 9.

273 We then use quantiles of \hat{N}_k^{boot} to represent confidence intervals and calculate
274 $\text{Var}(\hat{N})$ as $\text{Var}(\hat{N}^{boot})$.

275 **3.3 Extension to incorporate detection heterogeneity**

276 So far, we have not attempted to model detection heterogeneity outside of
277 individual covariates (e.g. through Eq. 7). However, it is common knowledge
278 that other factors can affect the distinctiveness of different animal groups
279 and impart additional heterogeneity leading to (often positive) dependence
280 in observer detection and thus negative bias in \hat{N} (Laake and Borchers, 2004;
281 Buckland et al., 2010; Burt et al., 2014).

282 In traditional MRDS applications (i.e. without movement and measure-
283 ment error), one approach is to correct for this bias by estimating observer
284 dependence parameters, typically through inclusion of an additional proba-
285 bility density function for observed distances in the likelihood (cf. Buckland
286 et al., 2010). However, inclusion of such a pdf in our likelihood appears prob-
287 lematic, as movement alters interpretation of distance distributions (Burt
288 et al., 2014). Alternatively, MacKenzie and Clement (2016) suggested that

observer dependence could also be included by modeling *conditional* detection probabilities; that is, including detection by one observer as a covariate for detection of the other. For instance, detection probabilities could potentially be written as a logit-linear function of an autocovariate $\xi_{io} = y_{i,3-o}$. We adapt this latter idea as a way to accommodate detection heterogeneity in data subject to movement and measurement error.

The major complication with using a detection autocovariate as a predictor in our case is that we are no longer able to say that an animal group with $y_{io} = 0$ was actually undetected by observer o . It could, for instance, have been detected but determined to not be in \mathcal{S} . As such, we view the autocovariate ξ_{io} as a latent variable. If $y_{io} = 1$, then $\xi_{i,3-i} = 1$ with certainty; however, if $y_{io} = 0$ we do not know whether $\xi_{i,3-i}$ is 0 or 1. Summing over each encounter history type (11,01, or 10) subject to uncertainty about ξ_{io} , we now need to calculate the probability of being observed by at least one observer as

$$\begin{aligned}
p_i^*(z_{i1}, z_{i2} | \mathbf{x}_i, \boldsymbol{\beta}, \boldsymbol{\phi}, \boldsymbol{\varphi}) &= p_{i1}(z_{i1} | \xi_{i1} = 1) \omega(z_{i1}, \mathcal{S}) p_{i2}(z_{i2} | \xi_{i2} = 1) \omega(z_{i2}, \mathcal{S}) + \\
&\quad p_{i1}(z_{i1} | \xi_{i1} = 0) \omega(z_{i1}, \mathcal{S}) (1 - p_{i2}(z_{i2} | \xi_{i2} = 1)) + \\
&\quad p_{i1}(z_{i1} | \xi_{i1} = 1) \omega(z_{i1}, \mathcal{S}) p_{i2}(z_{i2} | \xi_{i2} = 1) (1 - \omega(z_{i2}, \mathcal{S})) + \\
&\quad p_{i2}(z_{i2} | \xi_{i2} = 0) \omega(z_{i2}, \mathcal{S}) (1 - p_{i1}(z_{i1} | \xi_{i1} = 1)) + \\
&\quad p_{i2}(z_{i2} | \xi_{i2} = 1) \omega(z_{i2}, \mathcal{S}) p_{i1}(z_{i1} | \xi_{i1} = 1) (1 - \omega(z_{i1}, \mathcal{S})).
\end{aligned} \tag{10}$$

We adopt a similar construct for the observation model, $[\mathbf{y}_i, \mathbf{d}_i | \mathbf{z}_i, \boldsymbol{\theta}, \mathbf{x}_i]$,

305 recasting the likelihood contribution for animal group i as

$$(p_i^*)^{-1} \times \begin{cases} p_{i1}(z_{i1}|\xi_{i1} = 1)\omega(z_{i1}, d_{i1})p_{i2}(z_{i2}|\xi_{i1} = 1)\omega(z_{i2}, d_{i2}) & \text{if } y_{i1} = y_{i2} = 1 \\ p_{i1}(z_{i1}|\xi_{i1} = 1)\omega(z_{i1}, d_{i1})p_{i2}(z_{i2}|\xi_{i2} = 1)(1 - \omega(z_{i2}, \mathcal{S})) + \\ p_{i1}(z_{i1}|\xi_{i1} = 0)\omega(z_{i1}, d_{i1})(1 - p_{i2}(z_{i2}|\xi_{i2} = 1)) & \text{if } y_{i1} = 1, y_{i2} = 0 \\ p_{i2}(z_{i2}|\xi_{i2} = 1)\omega(z_{i2}, d_{i2})p_{i1}(z_{i1}|\xi_{i1} = 1)(1 - \omega(z_{i1}, \mathcal{S})) + \\ p_{i2}(z_{i2}|\xi_{i2} = 0)\omega(z_{i2}, d_{i2})(1 - p_{i1}(z_{i1}|\xi_{i1} = 1)) & \text{if } y_{i1} = 0, y_{i2} = 1. \end{cases} \quad (11)$$

306 Following these adjustments, we use the “symmetric” parameterization
 307 (MacKenzie and Clement, 2016) of observer dependence to include ξ_{io} in
 308 the logit-linear model for p_{io} . For instance, point independence (Laake and
 309 Borchers, 2004; Buckland et al., 2010) can be implemented by including an
 310 interaction between z_{io} and ξ_{io} with no main effect for ξ_{io} . Alternatively,
 311 limiting dependence (Buckland et al., 2010) can be implemented by including
 312 a main effect for ξ_{io} in addition to the interaction (MacKenzie and Clement,
 313 2016).

314 3.4 Goodness-of-fit

315 Goodness-of-fit is often summarized with χ^2 tests when distance data are
 316 binned (Burnham et al., 2004). However, this depends on having adequate
 317 sample sizes and homogeneous probabilities of detection within classes of
 318 animals. This latter requirement is problematic when detection probability

319 is written in terms of individual covariates. In order to get around this
 320 problem, we developed a simulation-based goodness-of-fit procedure similar
 321 in spirit to posterior predictive checks used in Bayesian analysis (e.g. Gelman
 322 et al., 2014). Our procedure consists of

- 323 1. Sampling $\boldsymbol{\theta}_k \sim [\boldsymbol{\theta}_{boot}]$,
- 324 2. Simulating new data $(\mathbf{d}_k, \mathbf{y}_i)$ from $[\mathbf{d}_k, \mathbf{y}_k | \mathbf{X}, \boldsymbol{\theta}_k]$.
- 325 3. Calculating a discrepancy measure $T(\mathbf{y}, \mathbf{d}, \boldsymbol{\theta})$ to compare the observed
 326 data to data simulated under the model.

327 For instance, we might compute the proportion of observations that occur
 328 in each distance bin when subset by various explanatory variables for our
 329 observed data and compare these to the distribution of proportions that we
 330 obtain by simulating data from our model when all assumptions are met. For
 331 some specific examples, see section 4.

332 3.5 Computing

333 We conducted MML inference in the R programming environment (R De-
 334 velopment Core Team, 2016). We have collated all code and data needed to
 335 recreate our analyses into an R package, `MRDSmove`. The package is currently
 336 available at <https://github.com/pconn/MRDSmove/releases> and will be
 337 archived on a publicly available data repository upon manuscript acceptance.

338 4 Analysis of waterfowl data

339 We fitted 12 MML models to our waterfowl data, varying by (1) movement
340 and measurement kernel type (Gaussian vs. Laplace), (2) observer depen-
341 dence type (none; point independence, or limiting independence), and (3)
342 whether or not moving individuals had a different distance function than
343 individuals that were not moving (Table 2). We calculated marginal AIC
344 to select between these models. We also fitted two Huggins-Alho (HA; Hug-
345 gins, 1989; Alho, 1990) models to our data using program MARK (White and
346 Burnham, 1999) via an RMark (Laake, 2013) interface. The HA models sup-
347 pose independent detection of observers and do not account for movement
348 or measurement error; abundance estimates are generated with a Horvitz-
349 Thompson-like procedure. The two HA models had the same structure but
350 differed in how data were formatted: in the first (HA1), distance was set
351 to d_{i1} whenever $d_{i1} \neq d_{i2}$; in the second (HA2), conflicting distance mea-
352 surements were averaged. For the HA models, detection probability was set
353 to the structure on the MML model with the best AIC score. All models
354 included the following predictors within the logit-linear model for detection
355 probability: group size, moving/not moving, observer (front vs. back), dis-
356 tance, distance², and an interaction between the distance effects and the
357 observer effects. The latter interaction was included because the view of the
358 first distance bin was partially obstructed for observer 2 and the distance
359 distribution appeared to peak further away from the plane (see Alisauskas

360 and Conn, 2017).

361 AIC strongly favored models with Laplace movement and measurement
362 error kernels over Gaussian kernels, although the impact of the functional
363 form of the kernel on resultant abundance estimates was quite small (Table
364 2). The highest ranked model had an interaction between distance and mov-
365 ing/not moving, suggesting different detection function shapes for moving vs.
366 stationary animals. However, pairwise model comparisons with and without
367 such an effect had similar AIC scores, so this effect was likely small. Point
368 and limiting independence models were favored over full independence mod-
369 els, suggesting some level of detection heterogeneity that was not captured
370 via gathered covariates.

371 The form of dependence had large effects on abundance estimates and
372 accompanying standard errors. In general, ‘li’ models produced the smallest
373 estimates, ‘fi’ models produced the next highest estimates, and ‘pi’ models
374 produced the highest estimates (Table 2). For instance, the top two mod-
375 els (including a pi model and fi model) were only 1.2 AIC units apart but
376 produced estimates of 3808 and 2993, respectively. The ‘pi’ models predict
377 increasing observer dependence with distance, while the ‘li’ models suggested
378 strongly negative observer dependence near the transect line which linearly
379 increased to positive dependence in distance bin 5 and beyond. This latter
380 type of observer dependence could occur if observers have different fields of
381 view and are likely to detect different animal groups close to the aircraft, but
382 are more likely to see the same animals (presumably the highly distinctive

ones) farther away.

Plots of movement and measurement error kernels (Fig 3) for the highest ranked model resembled raw data histograms (Fig 1). However, inclusion of movement and measurement error in the model did not appear to largely affect abundance estimates. For instance, HA1 and HA2 (the models without movement or measurement error) produced estimates of 1239 and 1278 waterfowl groups, respectively. By comparison, the 4 ‘fi’ models (which, like the HA models, presume conditional independence in observer detections), produced estimates of 1244-1259. In our example, it seemed far more important to account for different types of observer dependence. If an estimate were needed for management or conservation purposes, it would be wise to compute a model averaged estimate that incorporates uncertainty about the correction functional form of observer dependence (as well as attendant standard errors, which are much higher for ‘li’ and ‘pi’ models than for ‘fi’ models). We note that several of the ‘li’ models did not converge, a relatively frequent occurrence when fitting MRDS models Buckland et al. (2010); MacKenzie and Clement (2016).

To examine fit of our model to the data, we compared the properties of our MRDS dataset to 1000 data sets simulated from the highest ranked AIC model. In general, data sets simulated under our model had similar proportions of animals observed in the five distance bin classes as we observed in the field (Fig. 4). A notable exception was a tendency to overpredict the proportion of moving animals in distance bin 3. We are unsure of the reason for this

406 behavior, but have resisted the urge to consider more highly parameterized
 407 structures since a smooth decrease in the number of animals encountered as
 408 a function of distance is often expected a priori (Buckland et al., 2001), and
 409 it would be difficult to fit this particular “dip” in our distance data without
 410 violating monotonicity. Our model did a reasonable job in replicating the
 411 proportions of animals with each detection history type observed in the field.
 412 For instance, the number of ‘11’, ‘10’ and ‘01’ histories compiled for moving
 413 animals was 289, 261, and 179, respectively; these compared to 95% simula-
 414 tion intervals of (257,307), (227,276), and (173,219). For stationary animals,
 415 we observed 64 ‘11’, 92 ‘10’ and 79 ‘01’ histories compared to simulation
 416 intervals of (53,80), (74,103), and (68,95).

417 **5 Simulation studies**

418 We conducted two simulation studies to investigate bias, precision, and con-
 419 fidence interval coverage of our MML models and compared these to other
 420 MRDS analyses that do not account for movement and measurement er-
 421 ror. The first simulation study assumed independence between observer de-
 422 tections (i.e., no residual detection heterogeneity). The second experiment
 423 focused on performance of different approaches to estimation when hetero-
 424 geneous detection probabilities were simulated using random effects.

425 5.1 Simulation study I: Basic model performance

426 Our first simulation study was designed to look at estimator performance
427 over different movement and measurement error rates, and only considering
428 variation imparted by measurable covariates. For this study, we simulated
429 three different Gaussian movement kernel (Eq. 5) scenarios, corresponding
430 to (i) no movement ($\phi_1 = \phi_2 = 0$), (ii) symmetric movement ($\phi_1 = \phi_2 = 0.7$),
431 and (iii) asymmetric movement with much higher rates of movement away
432 from the transect line than towards the transect line ($\phi_1 = 0.5, \phi_2 = 1.5$).
433 We considered two levels of measurement error for each movement scenario:
434 no measurement error, or moderate measurement error ($\varphi = 0.5$).

435 In each of 500 simulations for the 6 movement and measurement error
436 scenarios, we conducted the following steps:

- 437 1. For each of $i \in 1, 2, \dots, 1000$ animals, we simulated an initial, latent
438 position z_{i1} in 10 equally sized distance bins using a uniform distribu-
439 tion.
- 440 2. After generating $m_i \sim \text{Bernoulli}(0.75)$ (so that approximately 75% of
441 animals were moving), we simulated z_{i2} using Eqn 3. For animals with
442 $m_i = 0$, we simply set $z_{i2} = z_{i1}$.
- 443 3. We simulated y_{io} and d_{io} using detection and measurement error mod-
444 els, where the first five distance bins were subject to observation (i.e.

445 $\mathcal{S} = \{\mathcal{Z}_1, \mathcal{Z}_2, \dots, \mathcal{Z}_5\}$). Detection probabilities were configured as

$$\text{logit}(p_{io}) = \beta_0 + \beta_1 m_i + \beta_2 z_{io} + \beta_3 z_{io}^2,$$

446 where $\beta_0 = 1$, $\beta_1 = 0.5$, $\beta_2 = 0.07$, and $\beta_3 = -0.09$.

- 447 4. We fit a sequence of three models to each such data set. These included
 448 (i) the movement and measurement error model proposed in this paper
 449 (configured with 8 latent distance bins), as well as the two Huggins-
 450 Alho models described in section 4. For all three estimation procedures,
 451 we used the same structure when estimating p_{io} as used to generate the
 452 data. For simulations where data were generated with $\phi = 0$ or $\varphi = 0$,
 453 we fixed the corresponding parameter in the estimation model to zero
 454 to prevent numerical errors.
- 455 5. For each model and data set, we tabulated bias, coefficient of variation
 456 (CV), 95% confidence interval coverage, and root mean square error
 457 (RMSE).

458 Note that in initial simulation work, we also fit movement and measurement
 459 error models with 10 latent distance bins, finding that results were almost
 460 identical to those with 8 latent distance bins (parameter estimates were often
 461 within 0.0001 of each other).

462 In general, bias from our new method was zero to slightly negative,
 463 while positive bias from the HA models could be substantial when move-

ment and/or measurement error occurred (up to 10%; Table 3). Precision and mean squared error were always better for the MML models than the HA models, with confidence interval coverage closer to nominal for most of the MML to HA model comparisons. However, coverage was less than nominal (85-91% for a 95% interval) for the MML models, suggesting that our bootstrap-based interval estimation procedure produces estimates of variance that are too small. Interestingly, HA1 estimates tended to have better properties (lower bias, better coverage, lower RMSE) than HA2 estimates, suggesting that taking distance values from observer 1 may be a better strategy than averaging distance values to resolve discrepancies if one chooses not to directly model movement and measurement error.

5.2 Simulation study II: Heterogeneous detection

In our second simulation scenario, we generated MRDS data for animals with highly heterogeneous detection probabilities in order to examine the utility of our proposed approach for coping with movement and measurement error in presence of extra detection heterogeneity. The main structure of our simulations was largely similar to the preceding section. We considered two different movement and measurement error scenarios corresponding to none ($\phi_1 = \phi_2 = \varphi = 0$) and to movement away from the survey line ($\phi_1 = 0$, $\phi_2 = 1.5$, $\varphi = 0.5$). For each of these scenarios, we considered two different expected sample sizes in the sampled area: $E(N) = 200$ and $E(N) = 1000$. In each combination of simulation implicates, we conducted 500 simulations

486 via following steps:

- 487 1. For each of $i \in 1, 2, \dots, 2E(N)$ animals, we simulated an initial, latent
488 position z_{i1} in 10 equally sized distance bins using a uniform distribu-
489 tion.
- 490 2. We generated m_i and z_{i2} as in Simulation Study 1.
- 491 3. We simulated d_{io} and y_{io} as in simulation study 1, once again using 5
492 observable distance bins. However, we used a half-normal model for
493 detection probability,

$$p_{io} = g_{io}^0 \frac{f(z_{io}|\mu = 1, \sigma_{io})}{f(1|\mu = 1, \sigma_{io})}$$

494 where g_{io}^0 gives detection probability in the first distance bin, and the
495 half normal model describes how detection probability declines in bins
496 that are farther away. These models were further parameterized as

$$\text{logit}(g_{io}^0) = \beta_0 + \beta_1 m_i, \text{ and}$$

$$\log(\sigma_{io}) = \alpha_0 + \alpha_1 m_i + \epsilon_i$$

497 where $\beta_0 = \alpha_0 = 1$, $\beta_1 = 0.5$, $\alpha_1 = 0.2$, and $\epsilon_i \sim \text{Uniform}(-0.7, 0.7)$.
498 The half-normal model seemed a reasonable way to implement point
499 independence (Laake and Borchers, 2004) using random effects (Fig.
500 5).

501 4. We fitted four models to each such data set. These included the same
502 three models from Simulation Study 1, and a fourth, marginal likeli-
503 hood model that attempted to estimate an observer dependence pa-
504 rameter in addition to movement and measurement error. Observer
505 dependence used a point independence specification (i.e. an interac-
506 tion between ξ_{io} and δ_{io}).

507
508 5. For each model and data set, we tabulated bias, coefficient of variation
509 (CV), 95% confidence interval coverage, and root mean square error
510 (RMSE).

511 Simulations suggested that the MML model with observer dependence
512 did a reasonable job at estimating abundance under all scenarios (Table 3)
513 even though the estimation model differed from the data generating model
514 (polynomial vs. half normal detection model; observer dependence effect vs.
515 random effects) . In particular, bias was low (-0.03 to 0.03) and 95% con-
516 fidence interval coverage was close to nominal (0.91 - 0.96) for all scenarios
517 examined. In contrast, bias of models ignoring observer dependence could be
518 considerable (up to -9%) with precision that was too high, leading to confi-
519 dence interval coverage that was too low (as low as 6% in one scenario). Not
520 surprisingly, bias was typically negative when ignoring observer dependence.
521 However, there was a mediating effect on bias whenever data were simulated
522 subject to both movement, measurement error, and observer dependence.

523 Since movement and measurement error alone induce positive bias, and ob-
524 server dependence alone produces positive bias, both processes combined
525 actually attenuate bias. For instance, HA models actually performed better
526 when both sources of bias were present than when either source of bias was
527 present singly.

528 **6 Discussion**

529 In this paper, we developed an approach to account for movement and mea-
530 surement error in MRDS analyses when observers independently record dis-
531 tances to animals, and when there is a binary covariate for moving/not mov-
532 ing. In simulation studies, our approach exhibited low bias and RMSE when
533 compared to a procedure that ignores movement and measurement error (the
534 latter resulted in positive biases of up to 10%). Importantly, we could conduct
535 estimation even in the face of residual detection heterogeneity, which seems
536 like a useful advance. Indeed, estimation of abundance in our field study was
537 much more sensitive to different functional forms for observer dependence
538 than it was to different functional forms for movement or measurement er-
539 ror.

540 Several avenues of future research are desirable. First, our bootstrap-
541 based estimates of variance resulted in confidence interval coverage that was
542 less than nominal in some of the simulation scenarios. A more robust way
543 of producing confidence intervals for Horvitz-Thompson-like abundance esti-

mates would be useful. Second, we have concentrated here on errors in dis-
 tances, but it is likely that other errors may occur (e.g. errors in group size
 determinations, individual covariates, species, etc.). Errors in species identifi-
 cation can be particularly problematic (see e.g. Conn et al., 2014) and should
 ultimately be addressed in multi-species surveys. Third, we have assumed
 additive measurement error in the present development; in some situations,
 multiplicative measurement error (whereby animals further away are subject
 to greater measurement error; Borchers et al., 2010) may make more sense.
 Finally, we have temporarily ignored the problem of expanding estimates
 from the surveyed area to some larger area of inference. One approach to
 expanding the scope of inference would be to include a sample inclusion prob-
 ability in the denominator of the Horvitz-Thompson estimator (i.e. eq. 9).
 Another approach would be to produce sequences of estimates for different
 surveyed areas (presumably sharing detection and movement/measurement
 error parameters between areas), and to use such estimates as responses for
 subsequent spatial modeling efforts (see e.g. Miller et al., 2013).

In this paper we conditioned on binary variables m_i for whether a de-
 tected group was moving or not. This approach let us separately estimate
 movement from measurement error by making the assumption that animals
 with $m_i = 0$ do not move. In other situations and study taxa (e.g. many ma-
 rine mammals), all animals may be moving in some fashion, and thus there
 may be insufficient data to separate these processes. In these circumstances,
 auxiliary data (e.g. animals with known location to estimate measurement

567 error; cf. Borchers et al., 2010) may be needed to implement our methods.

568 One exciting avenue for future research would be to expand our type
569 of modeling approach to allow movement within spatial capture-recapture
570 (SCR; see e.g. Borchers and Efford, 2008; ?) models. The generalized likeli-
571 hood structure of MRDS and SCR is actually very similar (Borchers et al.,
572 2015; Borchers and Marques, 2017), so incorporating movement could likely
573 be accomplished using the same construct in the paper (i.e. by viewing an
574 animals' locations as unobserved latent variables and integrating over all pos-
575 sible sequences of locations). The challenge would likely be a numerical one,
576 as space would need to be increased from one to two dimensions and over
577 a finer mesh, and the temporal dimension would need to increase from two
578 observers to a finite number of sampling occasions. One approach to high
579 dimensional integration would be to adopt a Bayesian perspective within a
580 data augmentation framework (Royle et al., 2007; Conn et al., 2012).

581 References

- 582 Alho, J. M. (1990), "Logistic regression in capture-recapture models," *Bio-*
583 *metrics*, 46, 623–635.
- 584 Alisauskas, R. T., and Conn, P. B. (2017), "Evaluating detectability of Arctic
585 waterfowl populations in double-observer helicopter surveys," , .
- 586 Borchers, D. L., and Efford, M. G. (2008), "Spatially explicit maximum

587 likelihood methods for capture–recapture studies,” *Biometrics*, 64(2), 377–
588 385.

589 Borchers, D. L., Laake, J. L., Southwell, C., and Paxton, C. G. M. (2006),
590 “Accommodating unmodeled heterogeneity in double-observer distance sam-
591 pling surveys,” *Biometrics*, 62, 372–378.

592 Borchers, D. L., and Marques, T. A. (2017), “From distance sampling
593 to spatial capture-recapture,” *AStA Advances in Statistical Analysis*,
594 doi:10.1007/s10182-016-0287-7.

595 Borchers, D. L., Stevenson, B. C., Kidney, D., Thomas, L., and Marques,
596 T. A. (2015), “A unifying model for capture–recapture and distance sam-
597 pling surveys of wildlife populations,” *Journal of the American Statistical*
598 *Association*, 110(509), 195–204.

599 Borchers, D. L., Zucchini, W., and Fewster, R. M. (1998), “Mark-recapture
600 models for line transect surveys,” *Biometrics*, 54, 1207–1220.

601 Borchers, D., Marques, T., Gunnlaugsson, T., and Jupp, P. (2010), “Esti-
602 mating distance sampling detection functions when distances are measured
603 with errors,” *Journal of Agricultural, Biological, and Environmental Statis-*
604 *tics*, 15(3), 346–361.

605 Buckland, S. T., Anderson, D. R., Burnham, K. P., Laake, J. L., Borchers,
606 D. L., and Thomas, L. (2001), *Introduction to Distance Sampling: Es-*

- 607 *timating the abundance of biological populations*, Oxford, U.K.: Oxford
608 University Press.
- 609 Buckland, S. T., Anderson, D. R., Burnham, K. P., Laake, J. L., Borchers,
610 D. L., and Thomas, L. (2004), *Advanced Distance Sampling* Oxford Uni-
611 versity Press.
- 612 Buckland, S. T., Laake, J. L., and Borchers, D. L. (2010), “Double-observer
613 line transect methods: Levels of independence,” *Biometrics*, 66, 169–177.
- 614 Burnham, K. P., Anderson, D. R., and Laake, J. L. (1980), “Estimation
615 of density for line transect sampling of biological populations,” *Wildlife*
616 *Monographs*, 72, 7–202.
- 617 Burnham, K. P., Buckland, S. T., Laake, J. L., Borchers, D. L., Marques,
618 T. A., Bishop, J. R. B., and Thomas, L. (2004), “Further topics in distance
619 sampling,” .
- 620 Burt, M. L., Borchers, D. L., Jenkins, K. J., and Marques, T. A. (2014), “Us-
621 ing mark–recapture distance sampling methods on line transect surveys,”
622 *Methods in Ecology and Evolution*, 5(11), 1180–1191.
- 623 Conn, P. B., Laake, J. L., and Johnson, D. S. (2012), “A hierarchical
624 modeling framework for multiple observer transect surveys,” *PLoS ONE*,
625 7, e42294.
- 626 Conn, P. B., Ver Hoef, J. M., McClintock, B. T., Moreland, E. E., Lon-
627 don, J. M., Cameron, M. F., Dahle, S. P., and Boveng, P. L. (2014),

628 “Estimating multi-species abundance using automated detection systems:
629 ice-associated seals in the eastern Bering Sea,” *Methods in Ecology and*
630 *Evolution*, 5, 1280–1293.

631 Gelman, A., Carlin, J. B., Stern, H. S., and Rubin, D. B. (2014), *Bayesian*
632 *data analysis, Third edition* Taylor & Francis.

633 Glennie, R., Buckland, S. T., and Thomas, L. (2015), “The effect of
634 animal movement on line transect estimates of abundance,” *PloS one*,
635 10(3), e0121333.

636 Huggins, R. M. (1989), “On the statistical analysis of capture-recapture ex-
637 periments,” *Biometrika*, 76, 133–140.

638 Laake, J. L. (2013), RMark: An R Interface for Analysis of Capture-
639 Recapture Data with MARK,, AFSC Processed Rep. 2013-01, Alaska Fish.
640 Sci. Cent., NOAA, Natl. Mar. Fish. Serv., Seattle, WA.
641 **URL:** <http://www.afsc.noaa.gov/Publications/ProcRpt/PR2013-01.pdf>

642 Laake, J. L., and Borchers, D. L. (2004), “Methods for incomplete detec-
643 tion at distance zero,” in *Advanced Distance Sampling*, eds. S. Buckland,
644 D. Anderson, K. Burnham, J. Laake, D. Borchers, and L. Thomas, Oxford,
645 U.K.: Oxford University Press, pp. 108–189.

646 MacKenzie, D. I., and Clement, D. (2016), “Accounting for Lack of Indepen-
647 dence and Partial Overlap of Observation Zones in Line-Transect Mark-

- 648 Recapture Distance Sampling,” *Journal of Agricultural, Biological, and*
649 *Environmental Statistics*, 21(1), 41–57.
- 650 Miller, D. L., Burt, M. L., Rexstad, E. A., and Thomas, L. (2013), “Spa-
651 tial models for distance sampling data: recent developments and future
652 directions,” *Methods in Ecology and Evolution*, 4, 1001–1010.
- 653 R Development Core Team (2016), *R: A Language and Environment for*
654 *Statistical Computing*, R Foundation for Statistical Computing, Vienna,
655 Austria. ISBN 3-900051-07-0.
656 **URL:** *http://www.R-project.org*
- 657 Royle, J. A., Chandler, R. B., Sollmann, R., and Gardner, B. (2013), *Spatial*
658 *capture-recapture* Academic Press.
- 659 Royle, J., Dorazio, R., and Link, W. (2007), “Analysis of multinomial models
660 with unknown index using data augmentation,” *Journal of Computational*
661 *and Graphical Statistics*, 16, 1–19.
- 662 White, G. C., and Burnham, K. P. (1999), “Program MARK: Survival es-
663 timation from populations of marked animals,” *Bird Study*, 46 Supple-
664 ment, 120–138.

665 TABLE CAPTIONS

666 Table 1: Definitions of fixed and estimated quantities for the MRDS
667 model incorporating movement and measurement error.

668 Table 2: Estimated abundance of waterfowl surveyed in northern Canada.
669 The first 10 models account for movement and measurement error and are fit-
670 ted via maximum marginal likelihood (MML), while the last two are Huggins-
671 Alho models that ignore movement and measurement error. MML models
672 are ranked by AIC; we also provide the number of parameters in each model
673 (k), log likelihood (LogL) at the MMLEs, the estimated number of waterfowl
674 groups \hat{G} , and the estimated number of waterfowl (\hat{N}). MML models varied
675 by the functional form of movement and measurement error kernels (Gaus-
676 sian vs. Laplace), the form of observer dependence (fi: full independence,
677 pi: point independence; li: limiting independence), as well as whether the
678 detection function included a distance:moving interaction. Note that we do
679 not report estimates for the two MML models that included both “limiting
680 dependence” and distance:moving interactions as these models did not con-
681 verge. For HA models, only estimated bird groups are reported owing to
682 software constraints. For reference, the number of detected bird groups was
683 964 and the total number of detected birds was 2666.

684 Table 3: Mean proportion relative bias (RelBias), coefficient of variation
685 (CV), 95% confidence interval coverage (Cover), and root mean squared error
686 (RMSE) for the two simulation studies. For the first simulation scenario,

687 “Configuration” gives values for movement (σ_1 and σ_2) and measurement
 688 error (φ) parameters; in simulation study 2, it indicates these parameters as
 689 well as expected population size in the surveyed area $N = 200$ or $N = 1000$.
 690 Three estimation models (Model) were fitted to each data set in simulation
 691 study 1: the maximum marginal likelihood (MML) model accounting for
 692 movement and measurement error, and two Huggins-Alho models which do
 693 not account for movement, measurement error, or observer dependence (HA1
 694 and HA2; described in the text). For simulation scenario two, we fitted an
 695 additional MML model that accounts for observer dependence (MMLd).

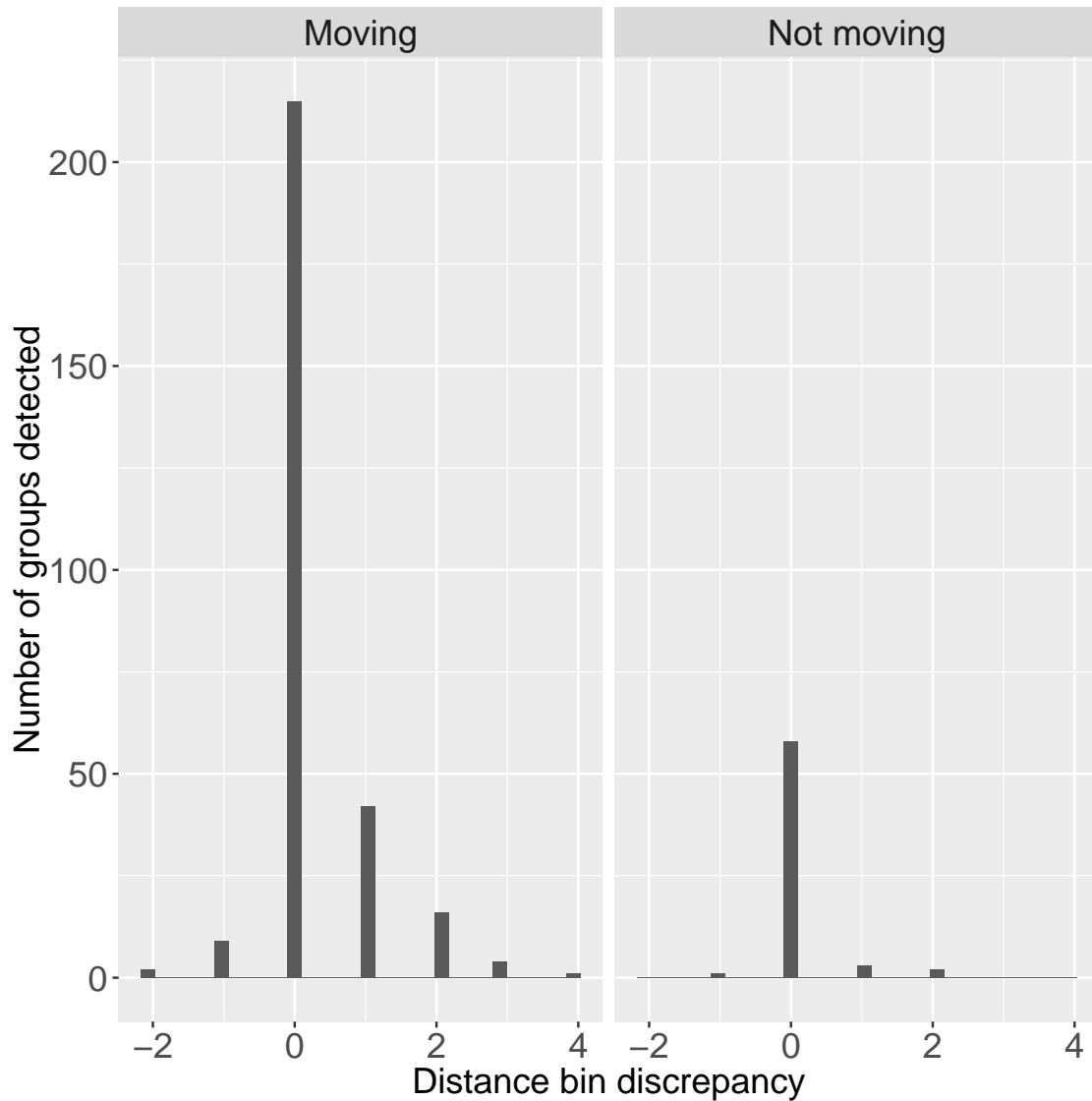


Figure 1: Distribution of distance bin discrepancies ($d_2 - d_1$) for bird groups encountered by both front and back seat observers in aerial surveys. For moving birds, the distance bin observed by the back observer tended to be further away than the bin observed by the front observer. Since the second observer invariably detected birds later than the front observer, this suggests responsive movement away from the aircraft.

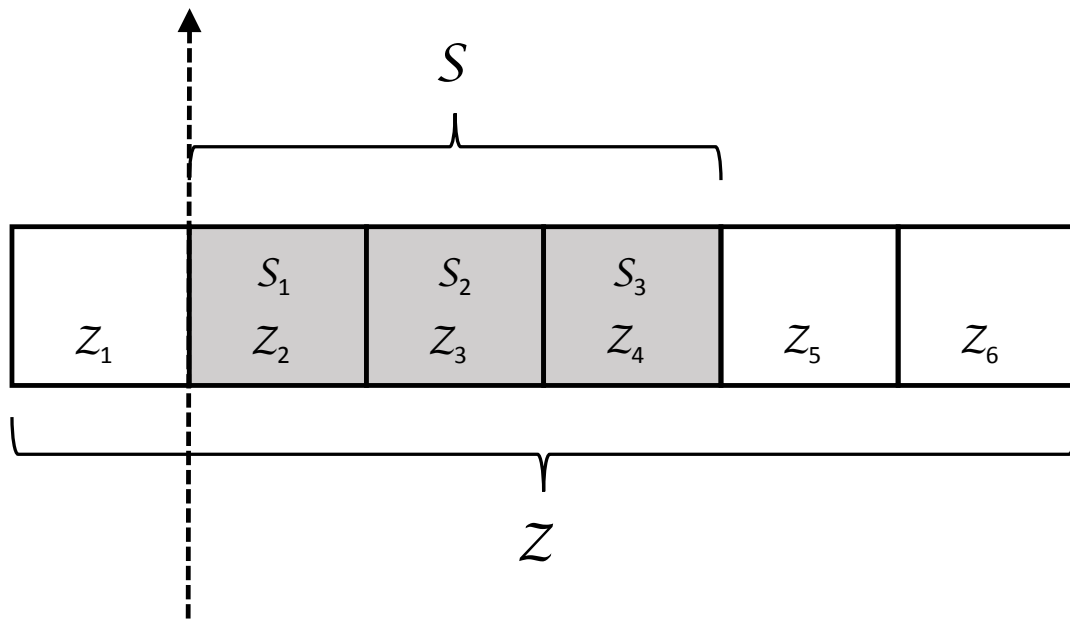


Figure 2: A depiction of observed (\mathcal{S}) and latent (\mathcal{Z}) distance bins that could potentially be used in analysis of a hypothetical mark-recapture distance sampling (MRDS) survey. In this example, only animals encountered in one of the three shaded distance bins to the right of the transect line (dashed line) are recorded; however, the state space is augmented with an additional three bins to account for possible animal movement and measurement error. In practice, the number of augmented distance bins that are needed will be a function of the magnitude of the movement and measurement error processes.

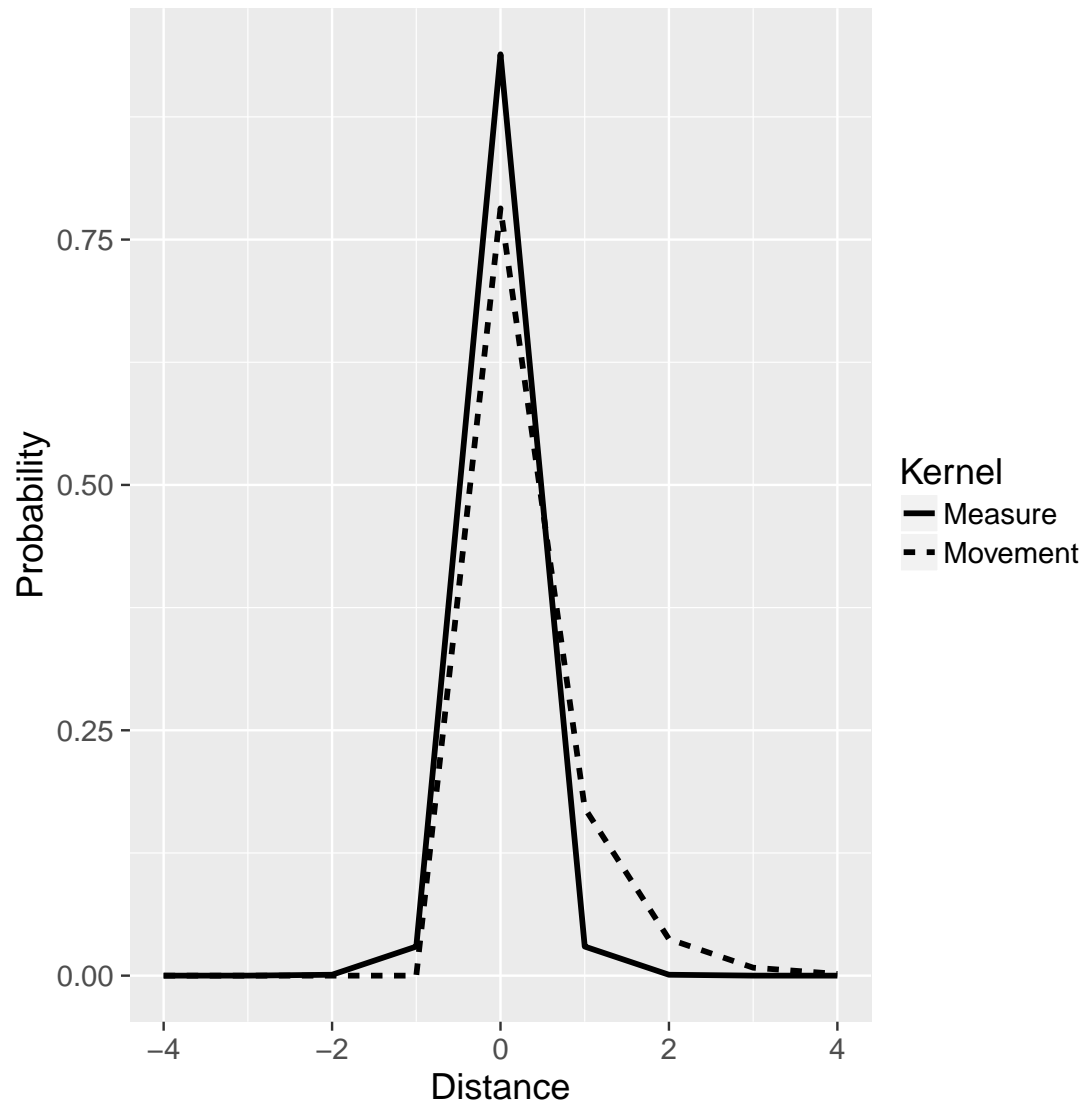


Figure 3: Estimated movement and measurement error kernels for waterfowl MRDS data from the highest ranked MML model.

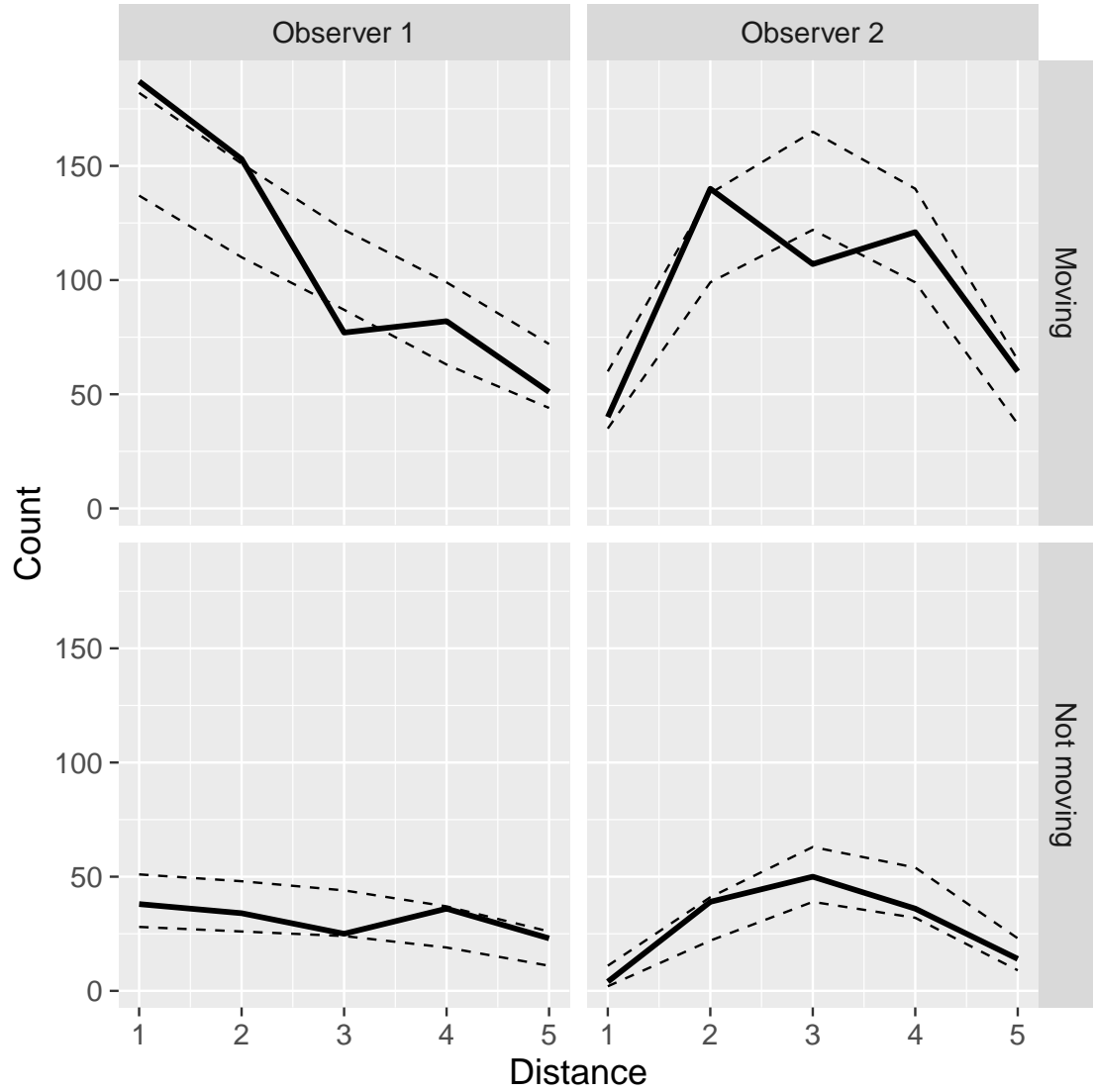


Figure 4: A plot of the number of observed and predicted waterfowl groups by observer and movement status. Observed data are given by the thick solid line, while the thin, dashed lines represent 2.5th and 97.5th quantiles of model-based simulations (including variance due to uncertainty of MML estimates).

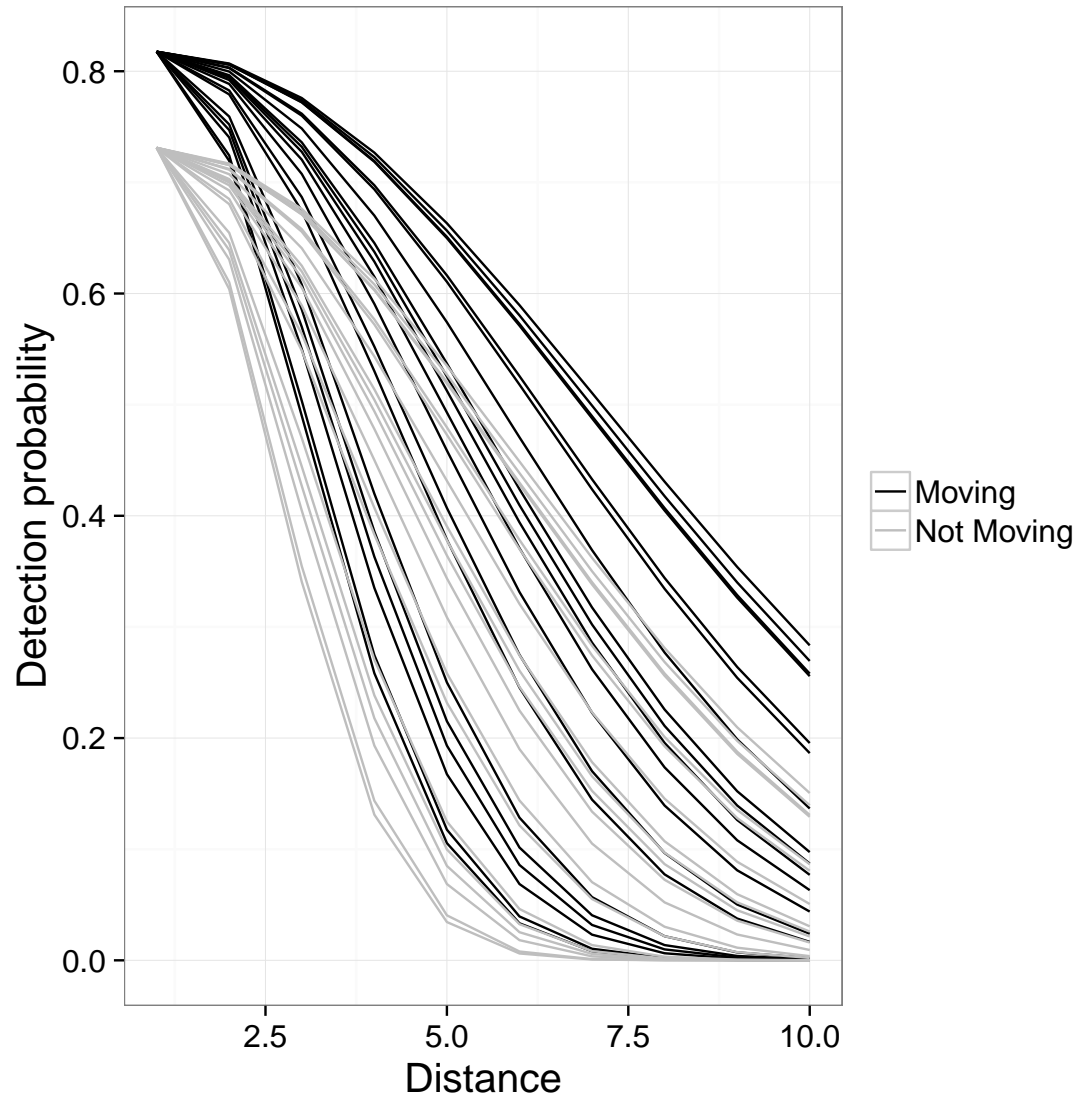


Figure 5: Detection probability for a random sample of 20 individuals from Simulation Study 2, where heterogeneity is incorporated via a random effect on the log of the standard deviation associated with a half-normal detection model. Detection probabilities are presented for cases where animals are moving (black lines) or not moving (gray lines)

Table 1:

Quantity	Definition
A. Fixed quantities	
n	Number of animals detected by at least one observer
y_{io}	Binary indicator for whether animal group i was detected by observer o
d_{io}	Distance bin recorded by observer o for animal group i (if recorded)
m_i	A binary indicator for whether animal group i was moving when observed (a single determination is made)
\mathbf{x}_i	A vector of covariates used to explain variation in detection probability for group i
g_i	Number of animals in group i (a single determination is made)
\mathcal{S}	The set of distance bins for which data are recorded, $\mathcal{S} = \mathcal{S}_1, \mathcal{S}_2, \dots, \mathcal{S}_{n_S}$
\mathcal{Z}	The set of latent distance bins used for modeling true animal locations, $\mathcal{Z} = \mathcal{Z}_1, \mathcal{Z}_2, \dots, \mathcal{Z}_{n_Z}$
π_j	Proportion of \mathcal{Z} covered by latent distance bin j
B. Parameters and functions of parameters	
z_{io}	True (latent) distance bin of group i when encountered by observer o
ξ_{io}	An indicator for whether or not observer $3 - o$ detected group i
δ_{io}	Perpendicular distance from the transect line to the midpoint of bin z_{io}
β	A vector of parameters governing logit-linear variation in detection probability
ϕ	Parameters governing animal movement
φ	Parameters governing distance measurement error
$p_{io}(z_{io})$	Probability that observer o detects group i given that the group is truly in distance bin z_{io}
$p_i^*(z_{i1}, z_{i2})$	Probability that at least one observer detects group i given the group is in distance bin z_{i1} at time 1 and z_{i2} at time 2
$\psi(z_{i1}, z_{i2})$	Probability that an animal that is in latent distance bin z_{i1} when it passes observer 1 will be in latent distance bin z_{i2} when it passes observer 2
$\omega(z, d)$	Probability that an animal group in distance bin z is recorded as being in distance bin d
$\omega(z, \mathcal{S})$	Probability that an animal group in distance bin z will have a recorded distance bin falling within \mathcal{S}
\mathbf{X}	A design matrix used to impart logit-linear structure on detection probabilities; note this will often include latent distance values, \mathbf{z}_i .
N	True abundance of animals in the surveyed area

Table 2:

Model	ΔAIC	k	LogL	$\hat{G}(\hat{\text{SE}})$	$\hat{N}(\hat{\text{SE}})$
MML.Laplace.pi.move	0.0	14	-2725.4	1519 (142)	3808 (302)
MML.Laplace.li	1.2	13	-2727.0	1122 (106)	2993 (222)
MML.Laplace.pi	3.2	12	-2729.0	1399 (99)	3562 (209)
MML.Laplace.fi	6.1	11	-2731.5	1244 (33)	3240 (73)
MML.Laplace.fi.move	6.7	13	-2729.8	1255 (35)	3261 (77)
MML.Gaussian.pi.move	55.5	14	-2753.2	1516 (149)	3800 (315)
MML.Gaussian.li	56.5	13	-2754.7	1130 (118)	3009 (247)
MML.Gaussian.pi	58.3	12	-2756.6	1394 (101)	3552 (212)
MML.Gaussian.fi	62.9	11	-2760.0	1248 (35)	3248 (80)
MML.Gaussian.fi.move	63.6	13	-2758.2	1259 (35)	3269 (79)
HA1	NA	10	NA	1239 (47)	NA
HA2	NA	10	NA	1278 (56)	NA

Table 3:

Configuration	Model	RelBias	CV	Cover	RMSE
A. Simulation study 1					
(0,0,0)	MML	0.00	0.03	0.91	214
(0,0,0)	HA1	0.01	0.04	0.95	532
(0,0,0)	HA2	0.01	0.04	0.95	529
(0.7,0.7,0)	MML	0.01	0.03	0.87	268
(0.7,0.7,0)	HA1	0.04	0.05	0.84	1144
(0.7,0.7,0)	HA2	0.06	0.05	0.80	1763
(0.5,1.5,0)	MML	-0.02	0.03	0.89	371
(0.5,1.5,0)	HA1	0.08	0.07	0.77	3086
(0.5,1.5,0)	HA2	0.07	0.07	0.84	2883
(0,0,0.5)	MML	0.00	0.03	0.91	245
(0,0,0.5)	HA1	0.01	0.05	0.95	490
(0,0,0.5)	HA2	0.03	0.05	0.93	740
(0.7,0.7,0.5)	MML	0.01	0.03	0.87	306
(0.7,0.7,0.5)	HA1	0.04	0.05	0.86	1237
(0.7,0.7,0.5)	HA2	0.07	0.06	0.75	2676
(0.5,1.5,0.5)	MML	-0.03	0.03	0.85	471
(0.5,1.5,0.5)	HA1	0.07	0.07	0.82	3045
(0.5,1.5,0.5)	HA2	0.10	0.08	0.77	4387
B. Simulation study 2					
(0,0,0), $N = 200$	MMLd	0.03	0.12	0.94	435
(0,0,0), $N = 200$	MML	-0.04	0.05	0.89	194
(0,0,0), $N = 200$	HA1	-0.06	0.06	0.83	312
(0,0,0), $N = 200$	HA2	-0.06	0.06	0.83	312
(0,1.5,0.5), $N = 200$	MMLd	-0.01	0.15	0.96	692
(0,1.5,0.5), $N = 200$	MML	-0.08	0.06	0.74	440
(0,1.5,0.5), $N = 200$	HA1	0.04	0.13	0.95	2581
(0,1.5,0.5), $N = 200$	HA2	0.00	0.12	0.92	921
(0,0,0), $N = 1000$	MMLd	0.03	0.05	0.91	2574
(0,0,0), $N = 1000$	MML	-0.05	0.02	0.33	3519
(0,0,0), $N = 1000$	HA1	-0.08	0.02	0.22	6315
(0,0,0), $N = 1000$	HA2	-0.08	0.02	0.22	6312
(0,1.5,0.5), $N = 1000$	MMLd	-0.03	0.05	0.94	3092
(0,1.5,0.5), $N = 1000$	MML	-0.09	0.02	0.06	8817
(0,1.5,0.5), $N = 1000$	HA1	-0.01	0.05	0.92	2607
(0,1.5,0.5), $N = 1000$	HA2	-0.03	0.04	0.84	3080